SPRFMO
South Pacific Regional Fisheries Management Organisation

9th MEETING OF THE SCIENTIFIC COMMITTEE

Held virtually, 27 September to 2 October 2021

SC9-HM03

Vorticity and Jack mackerel Catches

Peru

PO Box 3797, Wellington 6140, New Zealand
P: +64 4 499 9889 – F: +64 4 473 9579 – E: secretariat@sprfmo.int
www.sprfmo.int

SNP

INSTITUTO DEL MAR DEL PERU
IMARPE

IHMA

South Pacific Regional Fisheries Management Organisation
9th Meeting of the Scientific Committee
Held virtually, 27 September - 2 October 2021

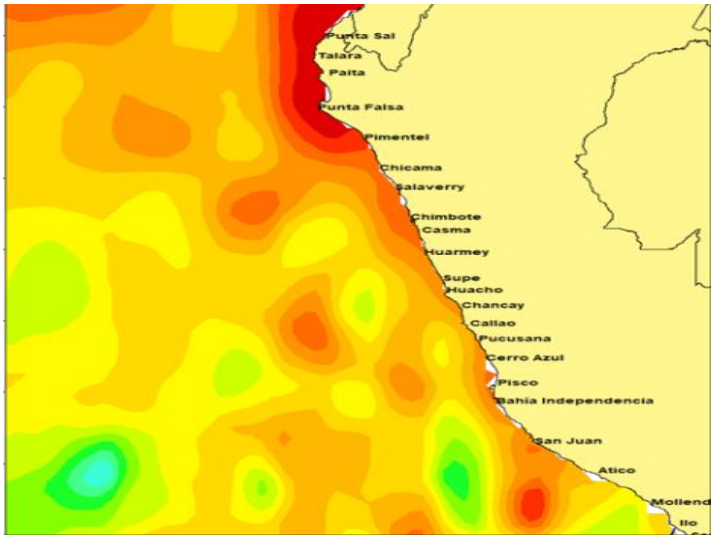

Relationship between oceanic vorticity and catches of jack mackerel (*Trachurus murphyi*) by the industrial purse-seine fishing fleet in Peruvian jurisdictional waters between 2011 and 2019

by

Susan Montero [(1)], Daniel Grados [(2)] and Mariano Gutiérrez [(3)]

[(1)] Pesquera Diamante, Lima, Perú
[(2)] Instituto del Mar del Perú (IMARPE), Callao, Perú
[(3)] Instituto Humboldt de Investigación Marina y Acuícola (IHMA), Lima, Perú

This report contains information on the Jack mackerel fish stock and fishery in Peruvian jurisdictional waters that, we reiterate, the delegation of Peru, in use of its discretionary powers, voluntarily provides for the purpose of information and support to the scientific research work within the Scientific Committee of the SPRFMO. In doing so, while referring to Article 5 of the Convention on the Conservation and Management of High Seas Fishery Resources in the South Pacific Ocean and reiterating that Peru has not given the express consent contemplated in Article 20 (4) (a) (iii) of the Convention, Peru reaffirms that the decisions and conservation and management measures adopted by the SPRFMO Commission are not applicable within Peruvian jurisdictional waters.

2021

SUMMARY

Surveying for fishing grounds makes it possible to direct fleets to the best available areas, in order to improve the efficiency and performance of fishing operations. However, the cost of these explorations is usually high, so it is necessary to generate predictive analyses that allow to increase the surveying and management efficiency of fishing operations. Besides, there are limited resources for in situ monitoring of vorticity in the ocean influencing the processes of convergence and divergence of the aggregation of nutrients, plankton and fish. To address these problems, the acoustic information collected aboard fishing vessels is valuable data that can be used to model the distribution of important species such as jack mackerel. Also, the habitat modeling of jack mackerel can be used in the assessment of the species for fisheries management purposes.

However, the strict fishing regulations in Peru, which prohibit the catch of juvenile jack mackerel (< 31 cm in total length), conditions the activities of the fleet, so that a study as the one described in this document, is only representative for the adult fraction of the population.

To study the relationship between ocean vorticity - which is characterized by meso and sub-mesoscale cyclonic and anticyclonic structures - and the distribution or availability of jack mackerel *(Trachurus murphy)*, it was used satellite information on sea level anomaly (SLA) and georeferenced catch data from industrial purse seine vessels operating in the Peruvian national waters between 2011 and 2019.

To study the relationship between sub-mesoscale structures and the local abundance of zooplankton and fish, it was used acoustic data collected during two scientific surveys performed by the Peruvian Marine Research Institute (IMARPE) along the Peruvian coast during 2011. From echograms it was automatically detected in high resolution the upper limit of the minimum oxygen zone (ULMOZ) in order to identify structures such as internal waves by using wavelet analysis.

Besides, the obtained results on the analysis of statistical and geographical correlation of jack mackerel catches with SLA indicated that catches were found invariably and positively correlated with the local abundance of macrozooplankton and with the location of the fronts between the cyclonic (divergent) and anticyclonic (convergent) eddies, so that ranges have been defined on the SLA values in order to be used in the habitat modeling of adult jack mackerel in Peru.

TABLE OF CONTENTS

1. INTRODUCTION

The marine Peruvian jurisdictional waters are under the strong influence of northern part of the Peruvian Current (PC), also known as Humboldt Current, represents only 0.1% of the world ocean area and produces about 10% of the world fish catch (Chavez, et al., 2008). Large-scale dynamics in the PC includes a complex dynamic on various time and space scales, which generate various surface and sub-surface currents, some of which are related to the South Pacific Anticyclone (Chaigneau et al., 2008). The PC is also periodically impacted by the development of warm (El Niño) and cold (La Niña) type of events.

However, in spite of the new knowledge that has been achieved about the dynamic processes that occur in the ocean, there are still few studies addressing the relationship between the distribution of fish and zooplankton as a function of the vorticity in the ocean. The vorticity is the result of the stratification and atmospheric circulation, wind flows, the earth rotation and the Coriolis effect, the coastal outline, and the morphology of the seabed. In particular, it is worth noting the formation and propagation in an east-west direction of cyclonic (divergent) and anticyclonic (convergent) eddies that can move a few hundred or thousand nautical miles during few months before becoming extinguished. In the southern hemisphere, cyclonic eddies rotate in a clockwise direction, and anticyclonic eddies rotate in an anti-clockwise direction. Eddies are cuasi circular structures that have an average radius of 75 to 100 nautical miles (Chaigneau et al., 2008; 2009); the cyclonic eddies have a typical depth of retention of 250 m, while the one for anticyclonic eddies is about 500 m. In the southeast Pacific, eddies usually originate near the western coast of South America, then propagate westward at a speed that increases with eddies located further north, varying from 5 cm/s at 20°S to 20 cm/s to 5°S (Chaigneau and Pizarro, 2005; Chaigneau et al., 2008; 2009).

It is known that ocean vorticity influences the processes of convergence and divergence in the aggregation of nutrients, plankton and fish (Habasque et al. 2013). Despite this knowledge, there are few studies that relate the geographical location of eddies with the local abundance of macrozooplankton and fish in the Peruvian Current. In the present case, this relationship has been studied for the case of the jack mackerel.

2. MATERIAL AND METHODS

2.1. Data used

2.1.1. Information on fishing sets and catches

Table 1 presents the main statistics of the fishing sets made between 2011 and 2019 by the industrial purse-seine fishing fleet of companies affiliated to the National Fisheries Society (SNP). The information between 2014 and 2017 has not been used since there were too few fishing sets on jack mackerel those years.

Table 1. Number of fishing sets and catches (tonnes) of jack mackerel by part of the industrial purse-seine fleet, by years and months, between 2011 and 2019, according to information from SNP. Data between 2014 and 2017 has been omitted as unrepresentative

Months	2011		2012		2013		2018		2019	
	Fishins sets	Catches (t)	Fishins sets	Catches (t)	Fishins sets	Catches (t)	Fishins sets	Catches (t)	Fishins sets	Catches (t)
January	212	20,693	1,095	78,290	134	9,118			239	32,139
February	171	15,890	147	10,576	459	20,960	63	3,627	464	50,645
March	508	49,732	138	15,584	366	14,679			158	12,404
April	458	28,055	496	46,044	43	3,702				
May	261	19,545			17	1,245				
June	185	15,440								
July	217	19,965					5	430		
August	257	23,925					141	12,011		
September	392	28,785					2	50		
October	126	6,367					130	12,581		
November							68	6,871		
December							5	160		
Total	2,787	228,397	1,876	150,495	1,019	49,704	414	35,730	861	95,188

2.1.2. Acoustic data

IMARPE's RAW files (echograms) were generated by Kongsberg SIMRAD scientific echosounders model EK60 operating at frequencies of 38 and 120 kHz aboard RV Olaya during acoustic surveys in summer and spring 2011. The acoustic sampling in both cases were systematic, the elementary sampling distance unit (ESDU) was 1 nm. In total, 6,339 and 6,503 ESDU were surveyed respectively.

2.1.3. VMS data

Vessel Monitoring System (VMS) data was provided by SNP. The number of data points (dp) on the location of industrial fishing vessels by years were: 2011 (149,128 dp), 2012 (37,570 dp), 2013 (58,576 dp), 2018 (70,929 dp) and 2019 (121,310 dp). The integrated VMS file contain the following information: date, time, longitude, latitude, heading (degrees), speed (knots) and SLA (cm).

2.1.4. SLA data

Satellite data on sea level anomaly (SLA) was obtained from Copernicus (https://marine.copernicus.eu/). SLA data is derived from the analysis of altimetry data, and generated from a combined analysis of the TOPEX/Poseidon, Jason1, ERS-1 and Envisat satellites distributed by the Copernicus Marine Environment Monitoring Service (CMEMS). SLA data was generated weekly according to availability of VMS and catch data. The SLA data files contain the next structure: date, time, longitude, latitude, and SLA (cm).

2.2. Methods

2.2.1. Identification of cyclonic and anticyclonic eddies from SLA satellite imagery

From satellite imagery, cyclonic and anticyclonic eddies can be identified by the contrast between areas with negative and positive SLA values. These zones are differentiated using color scales as shown in Figure 1.

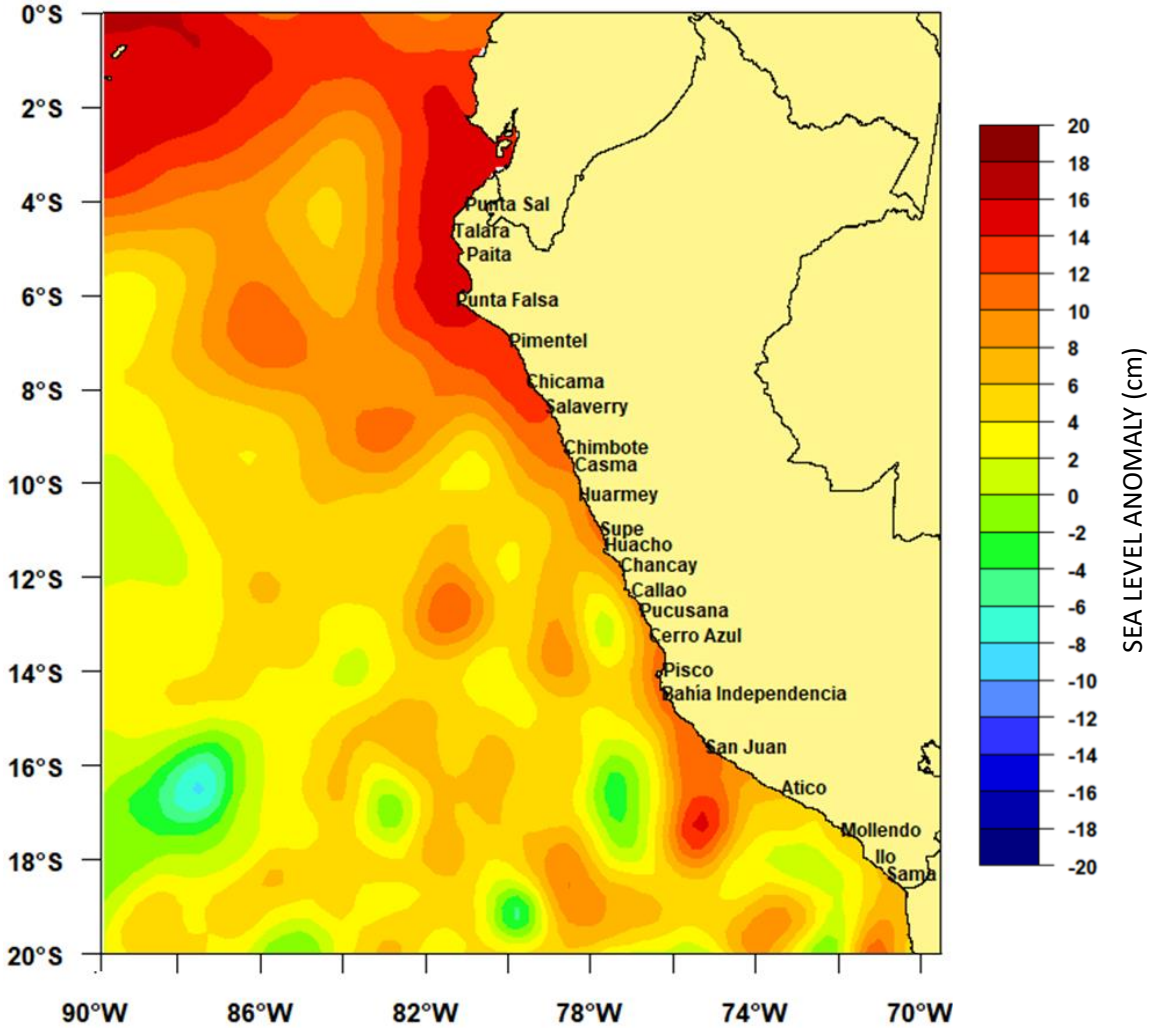

Figure. 1. Typical image of sea surface anomalies (SLA, cm). Cyclonic eddies, which rotate clockwise in the southern hemisphere, are related to negative SLA values (note the quasi-circular green and blue structures), while anticyclonic eddies, which rotate counterclockwise in the same hemisphere, are related to positive SLA values (quasi-circular red and orange structures).

2.2.2. GAM models

As the expected relationship between jack mackerel catches and SLA are nonlinear, a multivariate generalized additive model (GAM; Hastie and Tibshirani 1990) has been used with operators pre-designed in R language. A cubic regularizer was used to estimate the nonparametric functions. The response variable (jack mackerel catches) was previously transformed with decimal logarithms in order to reduce the bias of the estimate. In this way, GAM models were constructed for the logarithmic catches of jack mackerel, in order to find their relationships with SLA.

2.2.3. Wavelet analysis

The wavelet algorithms that have been used in this study are based on the methodology developed by Grados et al (2016), which uses information on the location of the upper limit of the oxygen minimum zone (ULOMZ). The ULOMZ is represented by a continuous line of variable depth at high resolution, which has been obtained from the acoustic data along all transects surveyed during the two IMARPE's surveys during 2011. We used the wavelet algorithm developed in Matlab ("WaveletsNCHS.m") by Grados et al (2016). The algorithm detects sub-mesoscale internal structures in the ocean based on the analysis of the variability along the ULOMZ.

2.2.4. Analysis of the acoustic abundance of macrozooplankton

The dominant group of macrozooplankton in the Peruvian Current are the euphausids and copepods (Ayón et al., 2008). An estimation of its abundance was developed by Ballon et al (2011) according to the acoustic properties of the "fluid-like" group (mainly euphausids and copepods). Although the shape of euphausids is more cylindrical than spherical, the two-frequency sphere model is considered appropriate when estimating the zooplankton biovolumes (Holliday & Pieper, 1995). To estimate the average size (radius of the sphere), the number of unsonified organisms and the biovolume of the macrozooplankton present in each cell was obtained by the method of the "Sv difference" between frequency responses at 38 and 120 kHz (Greenlaw, 1979; Ballon et al. 2011).

2.2.5. Detection of the vertical extension of the epipelagic zones

In the PC, the vertical extension of the epipelagic zone of zooplankton is limited by the presence of the minimum oxygen zone (MOZ) (Criales, et al., 2008; Ayón et al., 2008). For the purposes of this research, the depth of the ULMOZ was detected by using Echopen and Linea 98 algorithms developed by IMARPE and IRD on Matlab (MathWorks, USA).

3. RESULTS

3.1. Location of jack mackerel catches in 2011, 2012, 2013, 2018 and 2019 according to SLA values

VMS and georeferenced catch data on jack mackerel, have been subdivided into two periods according to the availability of information: from 2011 to 2013, and from 2018 to 2019. The catches of this portion of the fleet during the period from 2014 to 2017 were too few to be usable. The overlap of the SLA information, with catches obtained by the industrial fleet, allows to observe its probability of distribution. Figure 2 shows that catches of jack mackerel are mostly distributed along the edges and fronts between cyclonic and anticyclonic eddies. Based on this observation, we proceeded to demonstrate this relationship using GAM models and statistical analysis in order to calculate specific SLA ranges by years.

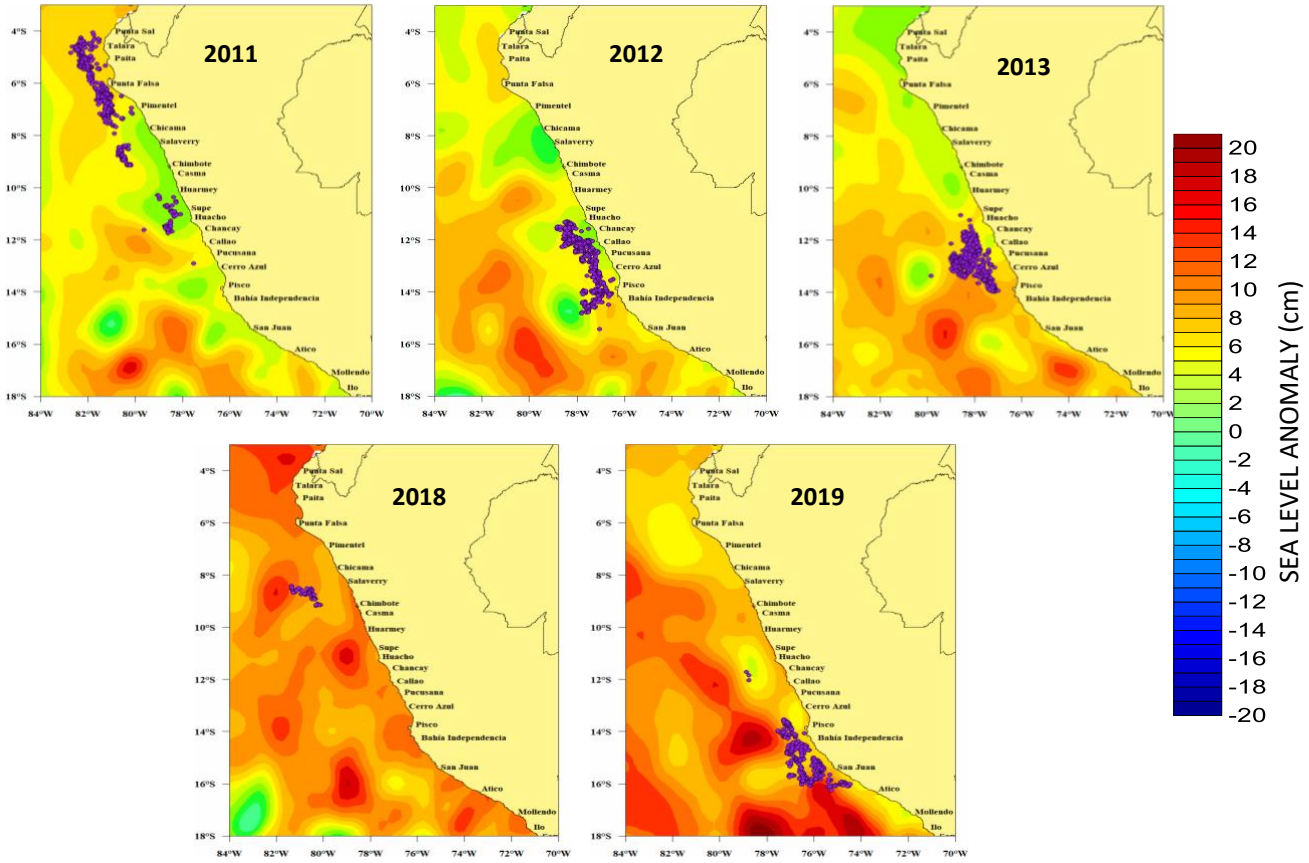

Figure 2. Overlap of jack mackerel catches obtained by part of the industrial purse-seine fleet, during summers, by years between 2011 to 2013 and 2018 to 2019 (represented by purple circles), on SLA images constructed as averages for February months in the indicated years. The quasi-circular red colors structures in the images correspond to convergence processes (anticyclonic eddies in the southern hemisphere), and yellow and green colors correspond to divergence processes (cyclonic eddies).

3.2. Generalized additive models (GAM) of SLA values (cm) regarding jack mackerel catches

Nonlinear relationships exist between catches of jack mackerel regarding sea level anomaly (SLA) values, as presented in Figure 3, where each panel shows the resulting GAM model to identify the range of SLA values observed according to catches.

The results of other GAM models show similar patterns for summer and fall seasons in the study years (2011 to 2013 and 2018 to 2019), but a slightly different pattern is observed during winter and spring seasons, although it should be noted that not every year there have been fishing seasons during July to December, either because the annual fishing quota granted by the government had already been caught, or because the fleet was dedicated to fishing for anchoveta. Also, the industrial fleet practically does not report jack mackerel catches between 2014 to 2017. During those years, El Niño conditions developed, and that during such warm years the availability of jack mackerel is usually reduced. However, in coastal areas (<10 nm), where the industrial fleet is not authorized to operate, the artisanal fleet has reported every year catches of jack mackerel, including 2014 to 2017.

The relationship between catches and SLA values for 2011 shows a positive trend during summer and autumn, with SLA values between 1 and 7 cm; during winter and spring a negative trend was observed, with SLA values between -4 and -2 cm. In 2012 a positive trend was obtained during summer and autumn, with SLA values ranging between 2 and 7 cm. In 2013 a positive trend was observed during summer and autumn, with SLA values between 2 and 6 cm. In 2018 no clear trend was observed. Finally, in 2019 a positive trend was observed during the summer season, with values SLA between 7 and 10 cm. Figure 3 and Table 2.

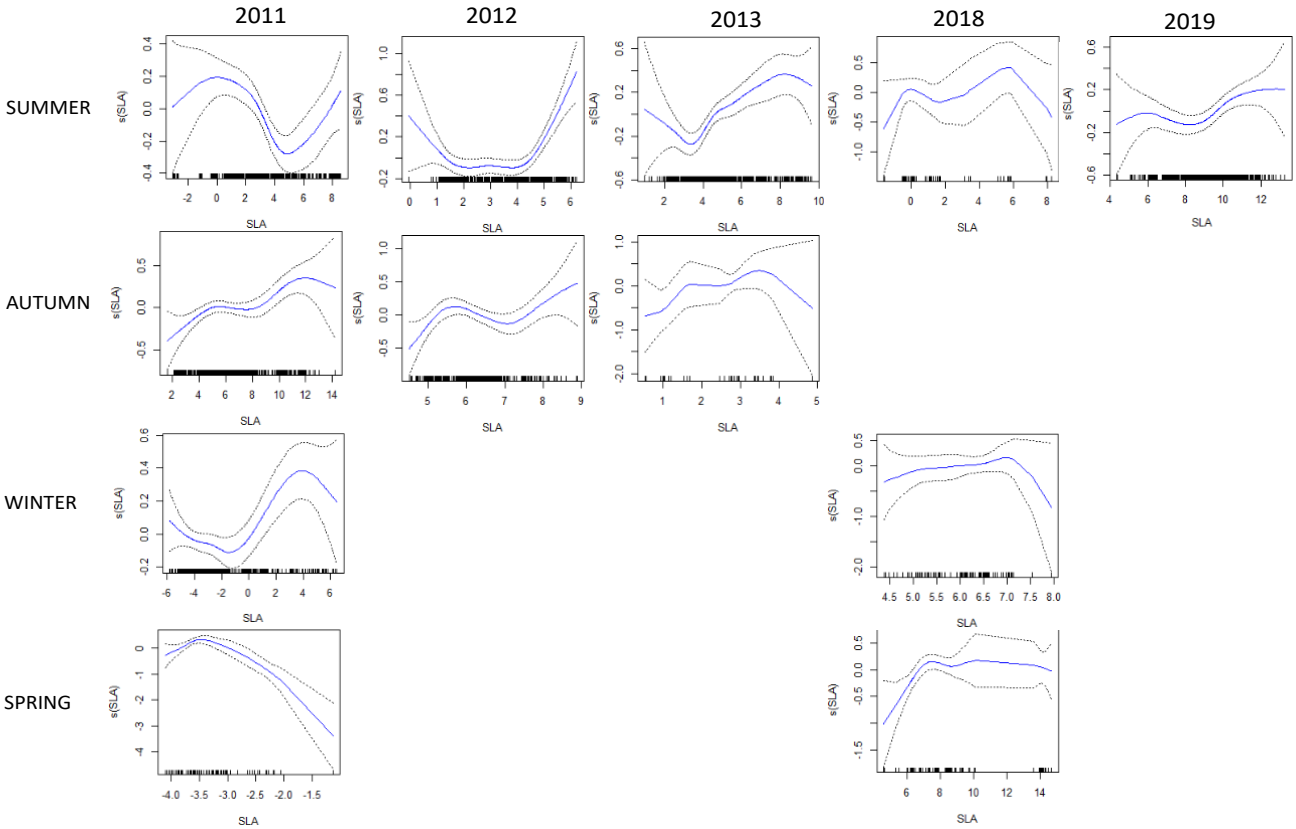

Figure 3. GAM models based on the logarithmic value of catches (blue lines) according to the sea level anomaly (SLA, in cm) by seasons between 2011 to 2013 and 2018 to 2019. The dotted gray lines represent the 95% confidence limits.

Table 2. Range of SLA values, for each year and season

Season	2011	2012	2013	2018	2019
Summer	1 to 5 cm	2 to 4 cm	4 to 6 cm	0 to 2 cm	7 to 10 cm
Autumn	4 to 7 cm	5 to 7 cm	2 to 3 cm		
Winter	-4 to -2 cm			6 to 7 cm	
Spring	-3 to -3 cm			7 to 9 cm	

3.3. Generalized additive models (GAM) of SLA values regarding VMS data

Figure 4 shows the GAM relationship between VMS data points - withing a vessel speed range from 0.2 to 1.6 knots under the assumption that lower speeds correspond to fishing sets - and SLA values. In 2011 a positive trend is observed during summer and autumn, with SLA values between 0.5 to 7 cm; during winter and spring a negative trend was observed, with SLA values ranging from -3.6 to -1.8 cm. In 2012 a positive trend was obtained during summer and autumn, with SLA values between 2 to 7 cm. In 2013 a positive trend was observed during summer and autumn, with SLA values between 2 to 6 cm. In 2018, no clear trend was observed. In 2019 a positive trend was observed during summer, with SLA values ranging between 6 and 10 cm.

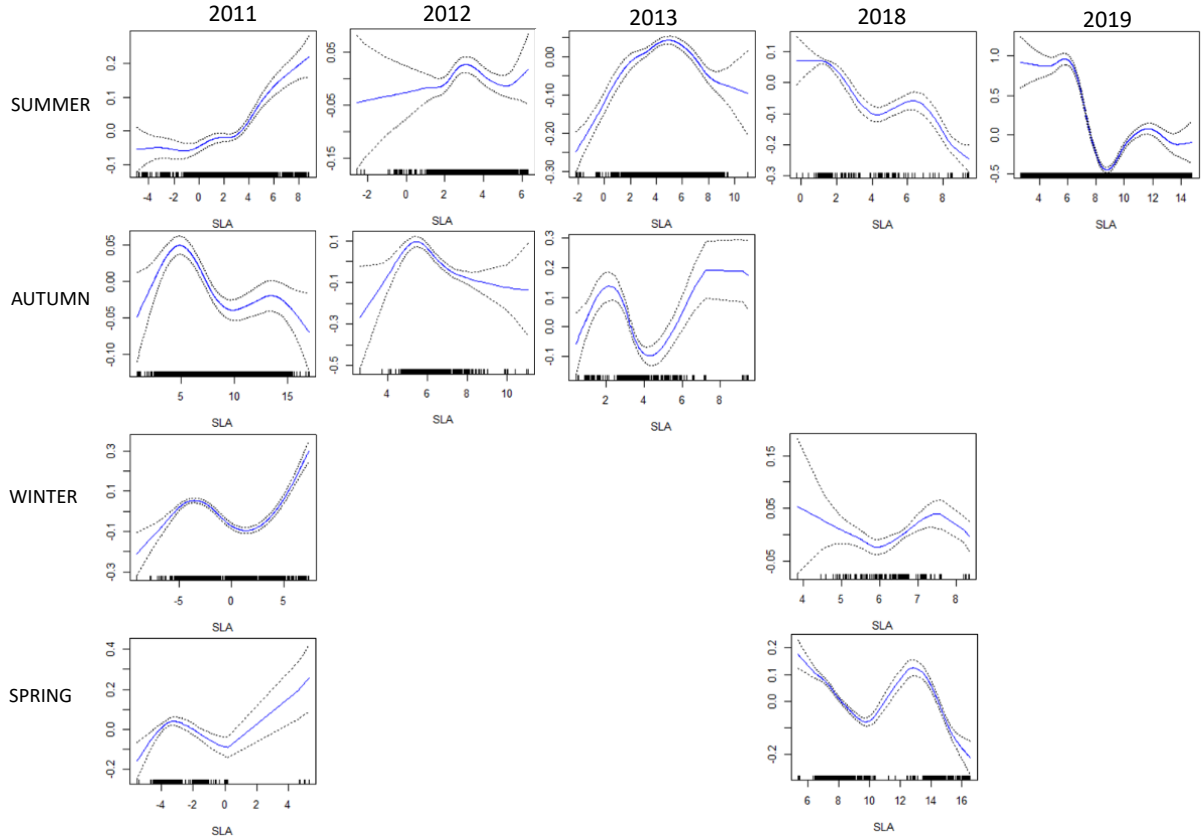

Figure 4. GAM models based on vessel speeds (blue lines) according to sea level anomaly (SLA, in cm), between 2011 to 2013 and 2018 to 2019. The dotted gray lines represent the 95% confidence limits.

3.4. Results of the classification of the structures for each survey

The results of the wavelet analysis and the classification of the structures for the summer (Cr. 1102-04) and spring (Cr. 1110-12) research surveys were obtained using the algorithm of Grados et al. (2016) (Figure 5). Up to 6 types of clusters of physical structures ranked according to their shape were found. Those six types were distinguished in three main categories of structures: (i) the internal wave category (called IW), which represents 55% of the structures detected and corresponds to types 1 and 2; (ii) the sub-mesoscale category (hereinafter referred as *Sub*) which represents 27% of the detected structures that corresponds to types 3, 4 and 5; and (iii) the mesoscale category (hereinafter referred as *Meso*) which represents 19% of the structures and corresponds to type 6. Table 3.

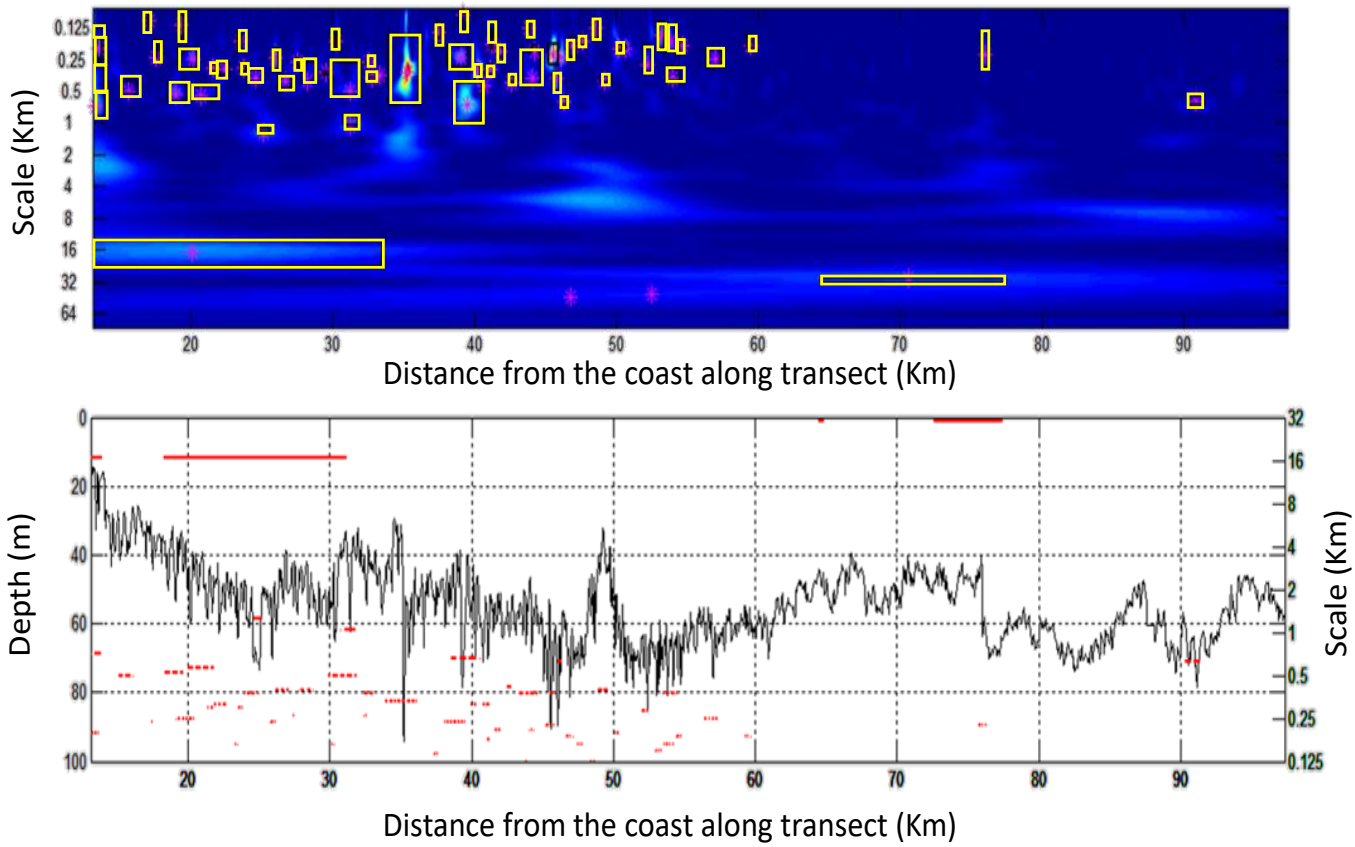

Figure 5. Sample of results on the detection of physical structures in the ocean along a 90 km long transect (top panel), where the yellow rectangles highlight the 6 types of clusters that have been detected. And fluctuation of the upper limit of the oxygen minimum zone (ULOMZ, oscillating black line) along the same transect (bottom panel), where the horizontal red segments correspond to the same cluster structures detected using the wavelet analysis.

Table 3. Characteristics (mean and standard deviation) of the 6 types of detected clusters. DS: downward deformation surface (m2); DC: distance from coast (Km); DSShelf: distance from shelf break (Km).

Cluster type	1	2	3	4	5	6
Width (km)	0.91 ± 0.35	0.75 ± 0.26	0.83 ± 0.56	2.15 ± 1.19	0.79 ± 0.35	1.00 ± 0.99
Height (m)	2.27 ± 1.08	1.82 ± 0.48	2.63 ± 0.67	2.58 ± 1.05	1.83 ± 0.50	1.99 ± 0.63
Depth (m)	47.36 ± 30.98	40.30 ± 26.41	48.86 ± 28.07	53.13 ± 35.15	47.90 ± 26.45	53.01 ± 18.22
DS (m2)	7.74 ± 1.77	5.09 ± 1.36	16.48 ± 3.68	10.61 ± 1.91	4.69 ± 1.02	6.33 ± 1.34
DC (km)	60.53 ± 48.32	55.16 ± 44.52	86.46 ± 26.49	69.73 ± 49.78	94.99 ± 33.55	60.04 ± 38.63
DShelf	37.83 ± 52.76	21.96 ± 50.93	41.75 ± 48.98	41.35 ± 55.98	38.36 ± 55.58	3.05 ± 34.20
Lat (°S)	11.52 ± 3.82	10.54 ± 3.73	10.59 ± 3.92	11.12 ± 3.83	10.51 ± 3.71	10.66 ± 3.71
Lon (°W)	77.66 ± 2.74	78.24 ± 2.68	78.61 ± 2.71	78.06 ± 2.62	78.76 ± 2.63	78.35 ± 1.98
% cluster	20%	35%	21%	5%	10%	9%

3.5. Correlation of the classified structures with schools detected during surveys

The location of the internal structure cluster types has been correlated with the nautical area scattering coefficient (NASC, m^2/nm^2) values by species groups. The groups have been formed according to similar distribution pattern: Group 1 (coastal): anchoveta (*Engraulis ringens*), white anchovy (*Anchoa nasus*), red squat lobster (*Pleuroncodes monodon*) and catfish (*Galeichthys peruvianus*); Group 2 (oceanic): jack mackerel (*Trachurus murphyi*) and chub (*Scomber japonicus*); Group 3: mesopelagic fishes; and Group 4: jumbo flying squid (*Dosidicus gigas*). The GAM correlation shows that: (1) group 1 has been found mostly in clusters types 3 and 4 that correspond to sub-mesoscale structures; (2) group 2 has been found in clusters type 2 and 3 that correspond to internal waves and sub-mesoscale structures; (3) groups 3 and 4 have been observed in type 3 clusters corresponding to sub-mesoscale structures. Figure 6.

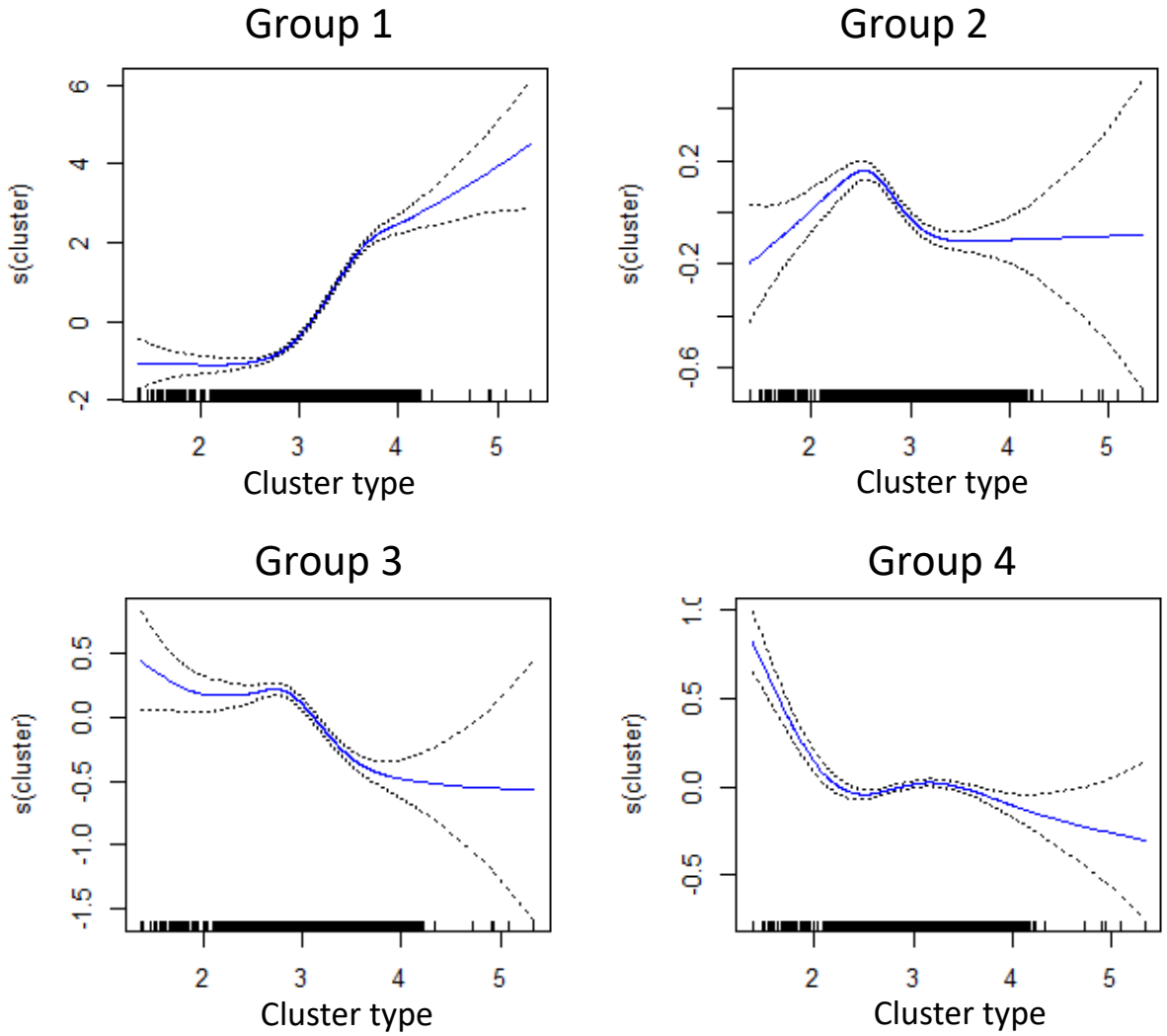

Figure 6. GAM analysis results based on the logarithmic value of NASC by groups of species (blue lines) according to cluster types. Notice the 95% limits (dotted grey lines) are wide for clusters type 1 and 6, therefore they are not shown on the X axis.

3.6. Relationship between the depth of the upper limit of the oxygen minimum zone (ULOMZ) and the acoustically measured biovolume

In figure 7 it is shown, in the left panel, the survey track of the acoustic assessment made during summer 2011 on the averaged SLA image. The right panel shows a sample of detection of ULOMZ (m) along a transect, where it is represented by a blue line on the left axis; the red line represents the biovolume (g/m^3) at the right axis. It can be noted that the biovolume of macrozooplankton increases as ULOMZ decreases, revealing a dynamic convergence process where plankton is aggregated along an internal structure of around 126 km long.

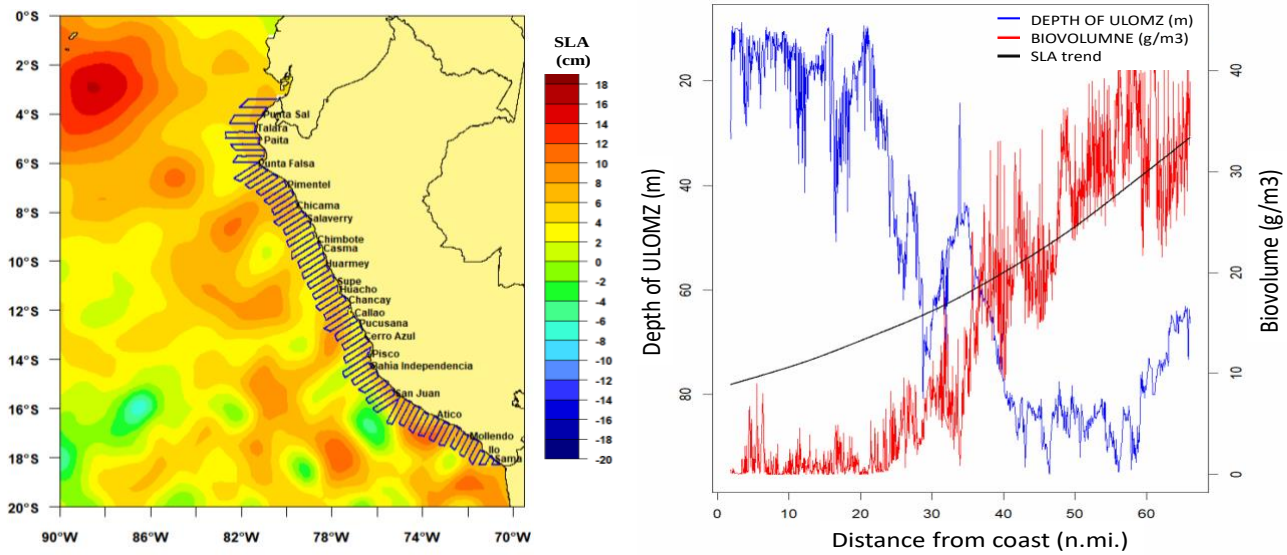

Figure 7. Left panel: overlap of an SLA image with transects surveyed by IMARPE during summer 2011 (indicated by black lines), where the red and orange areas correspond to convergence processes (anticyclonic eddies) and the light blue and green areas correspond to divergence processes (cyclonic eddies). Right panel: relationship between ULOMZ (m) and biovolume of macrozooplankton (g/m^3) along a sample transect (in n.mi.), where it is noted that the highest values of biovolume are reached at deeper ULOMZ, and the black line represents the SLA trend to increase its values when a convergence process is generated.

3.7. Pre-definition of probable fishing areas using information on sub-mesoscale structures

The purpose of this analysis is to observe the location of the detected convergent and divergent structures, since identifying the fronts between them might be useful in guiding a search strategy for possible fishing grounds using SLA imagery.

More than 9,000 physical structures were identified in the acoustic dataset for summer 2011. The classification analysis indicated the existence of six types of structures of sub-mesoscale. Figure 8 shows the images of the observed averaged SLA values obtained during the survey and, overlapped, the six types of clusters, where: type 1 (black points) and 2 (red circles); sub-mesoscale corresponds to cluster types 3 (orange circles), 4 (green circles) and 5 (blue circles); and the mesoscale cluster type 6 (light blue circles). The cyclonic eddies are shown in light bule to green colors; the anticyclonic eddies are observed in red to orange colors.

In Figure 8 it is also observed that the location of clusters type 1, 2, 4 and 6 is almost exclusively within the continental shelf (represented in the figure by a red line), while clusters type 3 and 5 are located both in and out the shelf break.

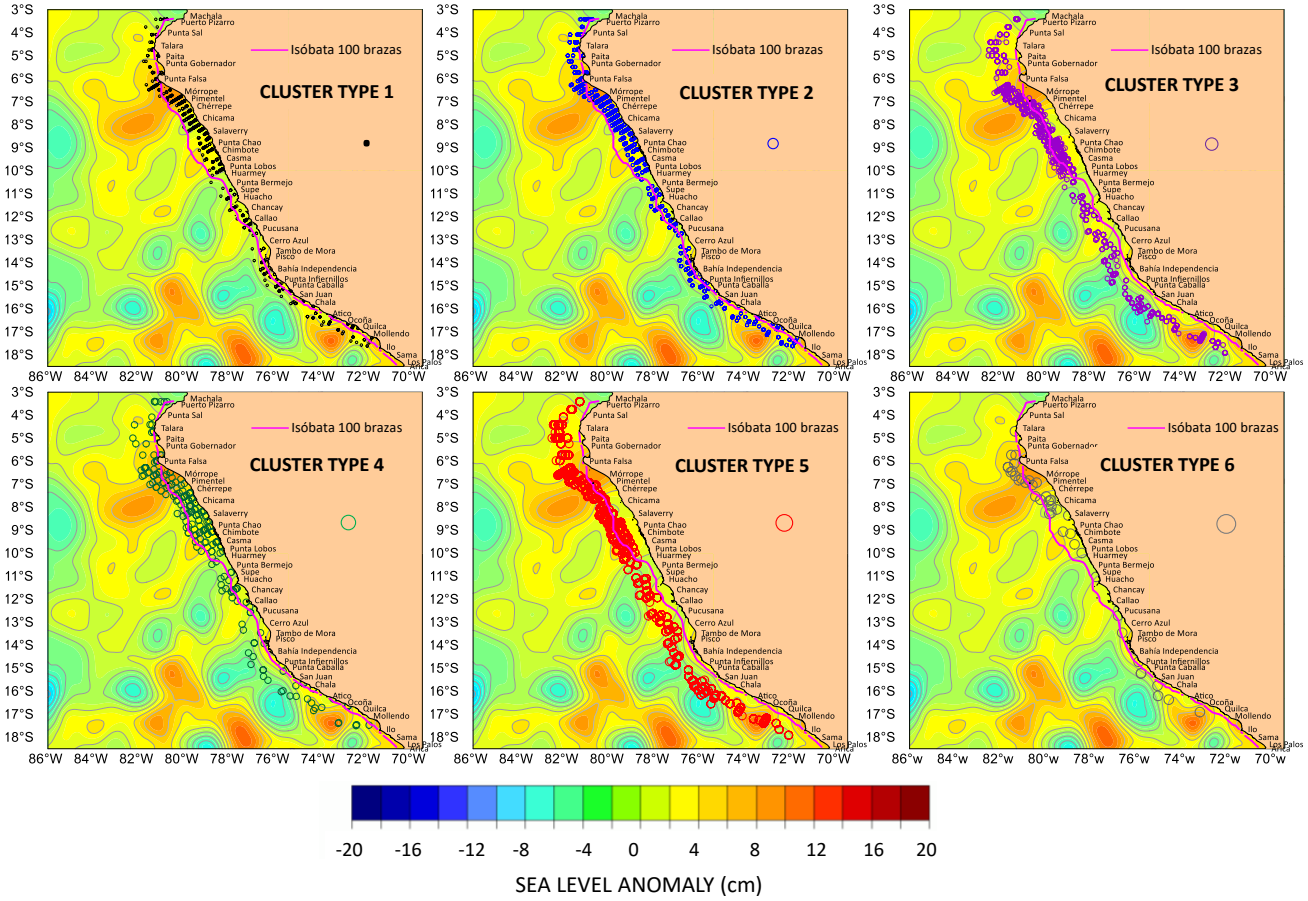

Figure 8. Sub-mesoscale structures (classified by clusters) superimposed on the averaged SLA image obtained during the summer acoustic survey 2011 (cyclonic eddies correspond to negative values while anticyclonic eddies correspond to positive values). Each panel contains the location of detected internal structures represented by different color and size symbols. Clusters type 1 are smaller and clusters type 6 are larger, as indicated in Table 3.

4. CONCLUSIONS

The results obtained explain the higher concentration of macrozooplankton and schools of fish, including jack mackerel in areas where the ULOMZ is deeper and coincident with internal structures of sub-mesoscale. The results also indicate that it is the zone of convergence between the cyclonic and anticyclonic eddies where the occurrence of fish is more frequent and of higher densities of macrozoplankton.

From the above it can also be concluded that:

- It is possible to identify and track the oceanic trajectories of converging (anticyclonic) and divergent (cyclonic) structures using sea surface anomaly (SLA) information as a guide for developing a search strategy for potential fishing areas, including jack mackerel. Edges of anticyclonic eddies along the shelf break generate better habitat

conditions for jack mackerel, since a positive relationship has been found between echo abundance of fish and macrozoopklancton on intermediate to positive SLA values.

- GAM modelling indicates that jack mackerel habitat during the summer is strongly related to the fronts between convergence and divergence structures, with a slightly positive trend towards anticyclonic eddies.
- The wavelet analysis showed that convergence and divergence eddies are related to the upwelling or downwelling, respectively, of the upper limit of the minimum oxygen zone (ULOMZ). It has been consistently observed that as ULOMZ became deeper the acoustic biovolume becomes higher and aggregated inside sub-mesoscale structures.
- It has been found through correlation analysis between acoustic values and location of the ULOMZ, that the group of species including jack mackerel and chub mackerel have a high degree of spatial correspondence with the so-called cluster type 2 (internal waves) and type 3 (sub-mesoscale structures).
- Internal waves (cluster types 1 and 2) are mostly located between the coast line and the shelf break, while the sub-messcale structures (clusters type 3, 4 and 5) and mesoscale (cluster type 6) are located at distances of more than 80 nm from the coast, both in and out the shelf break.
- The high correlation between jack mackerel catches and a specific range of SLA values allows us to conclude that it is possible to use SLA as an additional variable to improve the performance of the potential predictive habitat modeling of jack mackerel (MHPJ, Valdez et al 2015).

5. REFERENCES

Ayón, P., Swartzman, G., Bertrand, A., Gutiérrez, M., & Bertrand, S. (2008). Zooplankton and forage fish species off Peru: Large-scale bottom-up forcing and local-scale depletion. Progress in Oceanography, 79(2–4), 208–214. https://doi.org/10.1016/j.pocean.2008.10.023

Ballón, M., Bertrand, A., Lebourges-Dhaussy, A., Gutiérrez, M., Ayón, P., Grados, D., & Gerlotto, F. (2011). Is there enough zooplankton to feed forage fish populations off Peru? An acoustic (positive) answer. Progress in Oceanography, 91(4), 360–381. https://doi.org/10.1016/j.pocean.2011.03.001

Bertrand Arnaud, Grados D., Habasque Jérémie, Fablet R., Ballón M., Castillo R., Gutiérrez M., Chaigneau Alexis, Josse Erwan, Roudaut Gildas, Lebourges Dhaussy Anne, Brehmer Patrice. (2013). Routine acoustic data as new tools for a 3D vision of the abiotic and biotic components of marine ecosystem and their interactions. In : IEEE/OES Acoustics in Underwater Geosciences Symposium (RIO Acoustics). Piscataway : IEEE, 3 p. RIO Acoustics 2013, Rio de Janeiro (BRA), 2013/07/24-26. ISBN 978-1-4799-0362-7. Identifiant IRD : fdi:010064376

Chavez, F., Bertrand, A., Guevara-Carrasco, R., Soler, P., & Csirke, J. (2008). The northern Humboldt Current System: Brief history, present status and a view towards the future. Progress in Oceanography, 79(2–4), 95–105. https://doi.org/10.1016/j.pocean.2008.10.012

Chaigneau, A., & Pizarro, O. (2005). Surface circulation and fronts of the South Pacific Ocean, east of 120°W. Geophysical Research Letters, 32(8), 1–4. https://doi.org/10.1029/2004GL022070

Chaigneau, A., Gizolme, A., & Grados, C. (2008). Mesoscale eddies off Peru in altimeter records: Identification algorithms and eddy spatio-temporal patterns. Progress in Oceanography, 79(2–4), 106–119. https://doi.org/10.1016/j.pocean.2008.10.013

Chaigneau, A., Eldin, G., & Dewitte, B. (2009). Eddy activity in the four major upwelling systems from satellite altimetry (1992-2007). Progress in Oceanography, 83(1–4), 117–123. https://doi.org/10.1016/j.pocean.2009.07.012

Criales-Hernández, M. I., Schwamborn, R., Graco, M., Ayón, P., Hirche, H. J., & Wolff, M. (2008). Zooplankton vertical distribution and migration off Central Peru in relation to the oxygen minimum layer. Helgoland Marine Research, 62(2 SUPPL.1), 85–100. https://doi.org/10.1007/s10152-007-0094-3

Grados, D., Bertrand, A., Colas, F., Echevin, V., Chaigneau, A., Gutiérrez, D.,... Fablet, R. (2016). Spatial and seasonal patterns of fine-scale to mesoscale upper ocean dynamics in an Eastern Boundary Current System. Progress in Oceanography, 142, 105–116. https://doi.org/10.1016/j.pocean.2016.02.002

Greenlaw C. (1979) Acoustical estimation of zooplankton populations. Limnology and Oceanography 24(2): 226-242.

Hastie, T. & Tibshirani, R. (1990), Generalized Additive Models, Chapman and Hall.

Holliday D. V. & Pieper R. E. (1995) Bioacoustical oceanography at high frequencies. ICES Journal of Marine Science 52: 279-296.

Simmonds, J.E. and Maclennan, D.N. (2005) Fisheries Acoustics Theory and Practice, 2nd edn. New York: Chapman & Hall

Valdez Mego, C. (s.f.). Modeling of the potential habitat of horse mackerel (*Trachurus murphyi*) validated through captures and acoustic information from industrial fishing vessels. Lima - Peru: 2017.